Supplementary Information (SI) for Nanoscale.

Unique NiCo Bimetal-Boosting 98% CH_4 Selectivity and High Catalysis Stability for Photothermal CO_2 Hydrogenation

Yubin Zheng [a‡], Zhe Lu [b‡], Zhisheng Shi [c*], Lu, Wang[b], Shuyuan Yang[d], Runzhi Cao[a], Gao Wa [e*], Xin Zhou [df*], Yong Yang [g], Chong Sheng [a], Yong Zhou [a,b,*] and Zhigang Zou[a,b]

[a] *Key Laboratory of Modern Acoustics (MOE), Institute of Acoustics, School of Physics, Jiangsu Key Laboratory of Nanotechnology, Eco-materials and Renewable Energy Research Center (ERERC), National Laboratory of Solid-State Microstructures, Collaborative Innovation Center of Advanced Microstructures, Nanjing University, Nanjing, Jiangsu 210093, P. R. China. E-mail: zhouyong1999@nju.edu.cn.*

[b] *School of Science and Engineering, The Chinese University of Hong Kong, Shenzhen, Shenzhen 518172, P. R. China.*

[c] *School of Chemical and Environmental Engineering, Anhui Polytechnic UniversityWuhu, Anhui, 241000, P. R. China. E-mail: shizhisheng@ahpu.edu.cn.*

[d] *College of Environment and Chemical Engineering, Dalian University, Dalian 116622, P. R. China.*

[e] *School of Physical Science and Technology, Tiangong University, Tianjin 300387, P.R. China. E-mail: gaowa@tiangong.edu.cn.*

[f] *Interdisciplinary Research Center for Biology and Chemistry, Liaoning Normal University, Dalian 116029, P. R. China. Email: xzhou@lnnu.edu.cn.*

[g] *School of Chemistry and Chemical Engineering, Nanjing University of Science and Technology, Nanjing 210094, China. yychem@njust.edu.cn.*

‡*These authors contributed equally to this work and should be considered co-first authors.*

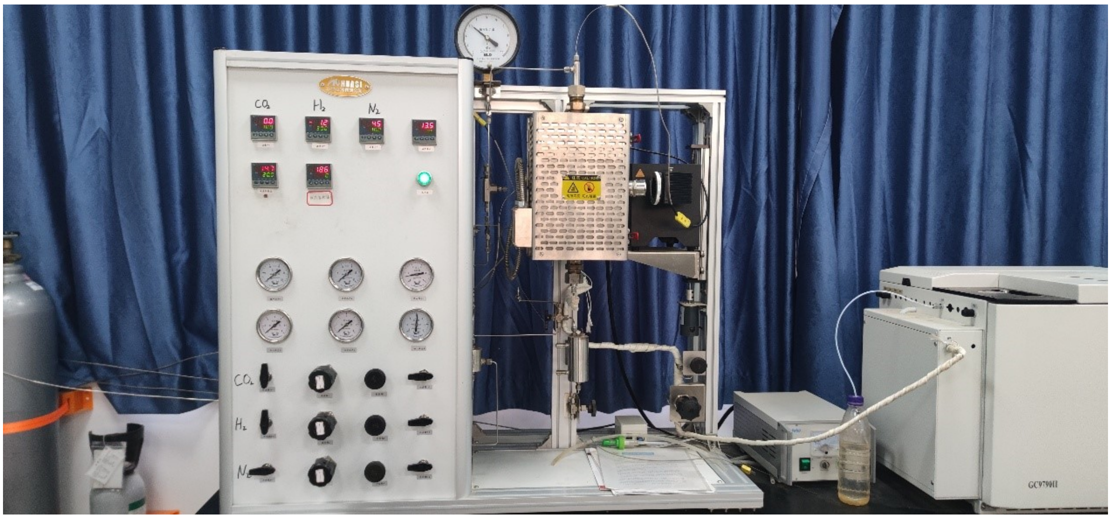

Figure S1. Photographic picture of photothermal catalytic reaction devices.

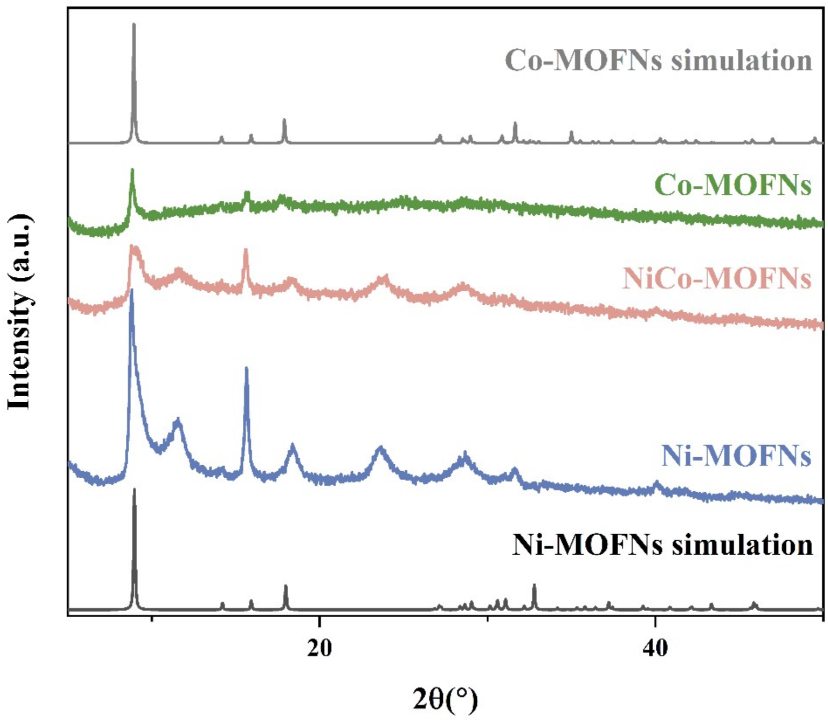

Figure S2. PXRD patterns of Ni-MOFNs, Co-MOFNs, and NiCo-MOFNs, as compared to the corresponding powder pattern.[1]

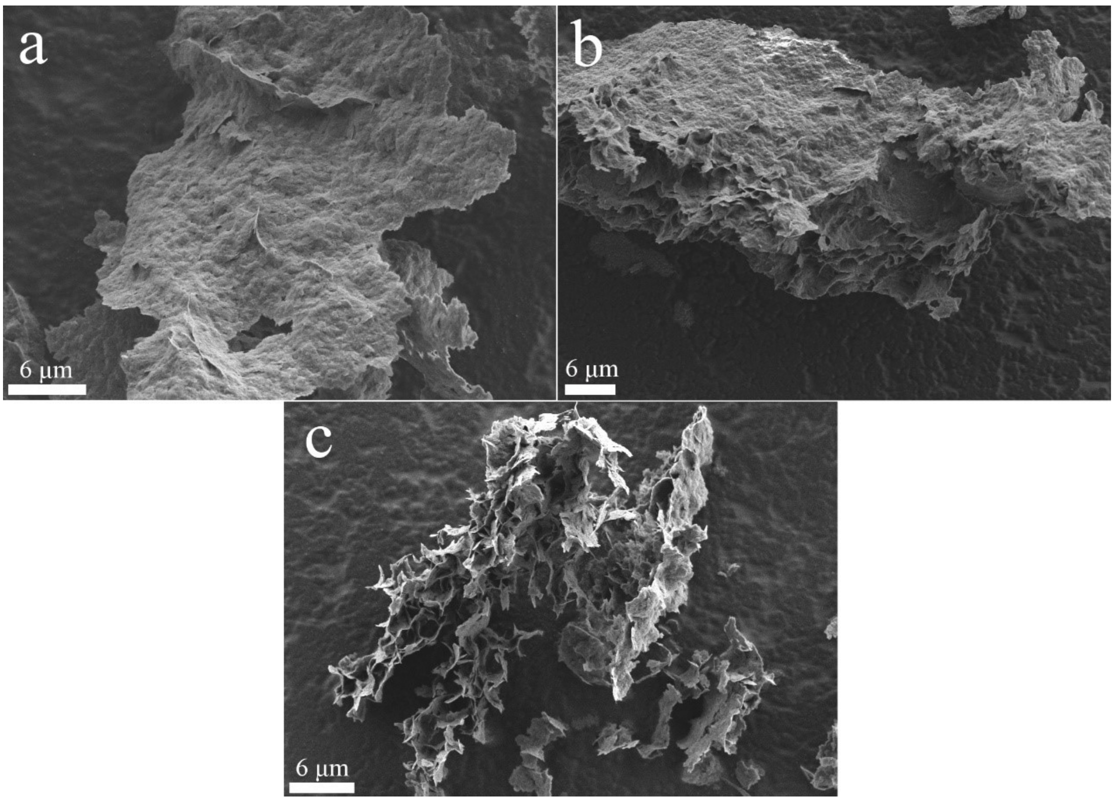

Figure S3. SEM images of a) Ni-MOFNs, b) Co-MOFNs, and c) NiCo-MOFNs.

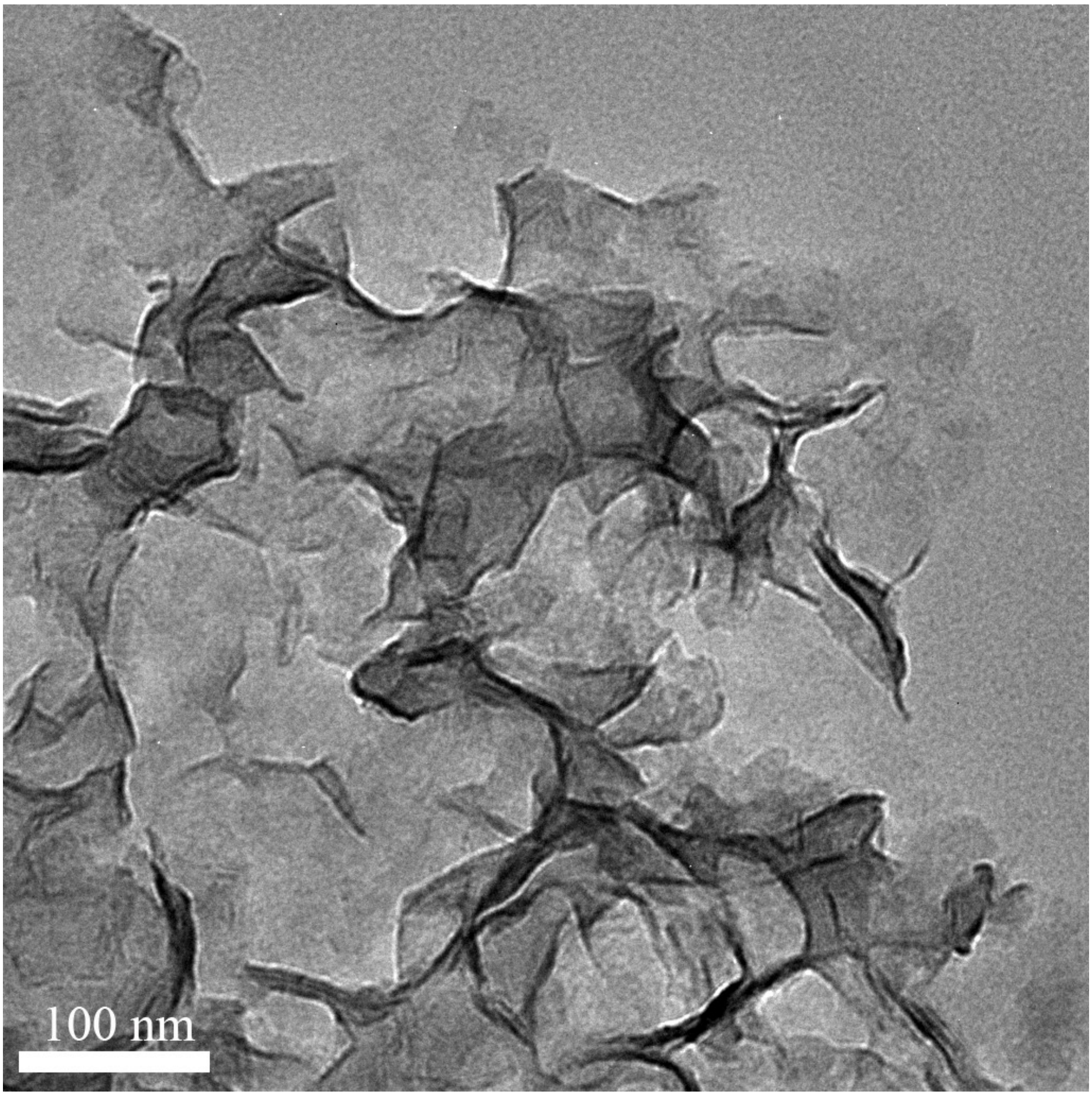

Figure S4. TEM image of NiCo-MOFNs.

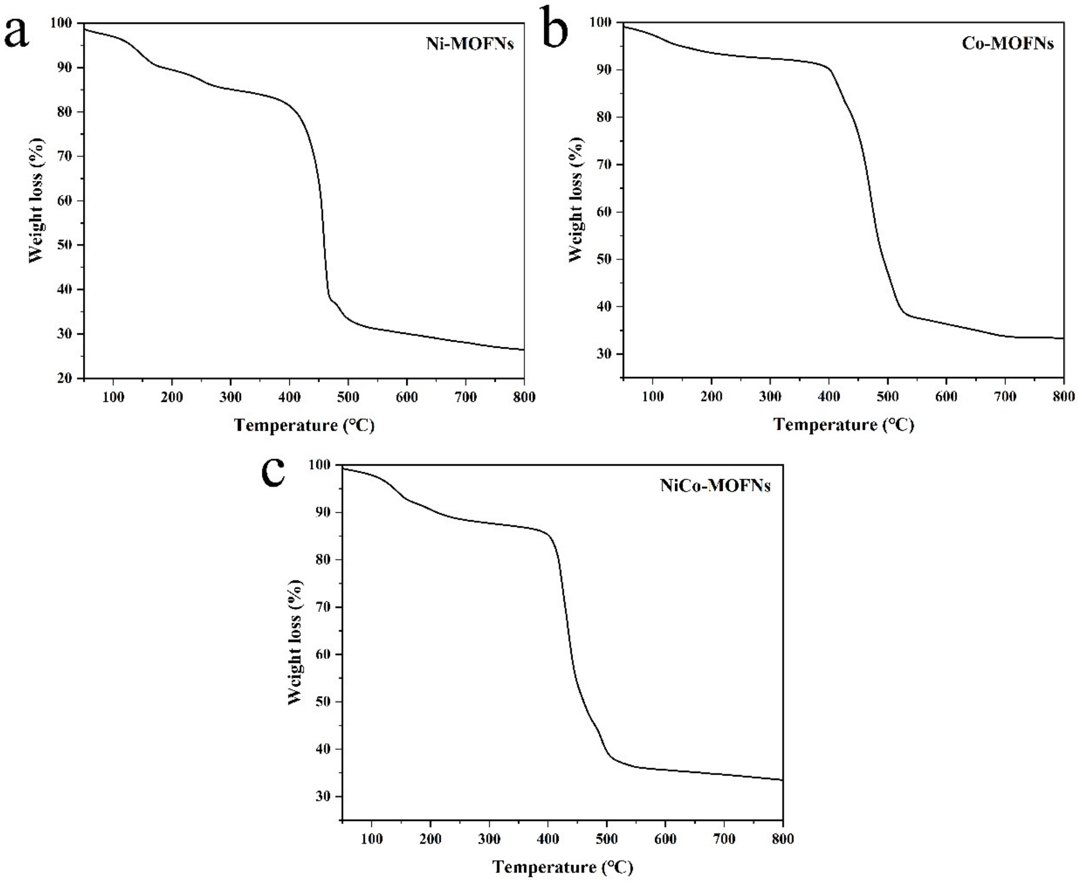

Figure S5. TGA curve of a) Ni-MOFNs, b) Co-MOFNs, and c) NiCo-MOFNs in N_2 atmosphere with a heating rate of 5 °C min^{-1}.

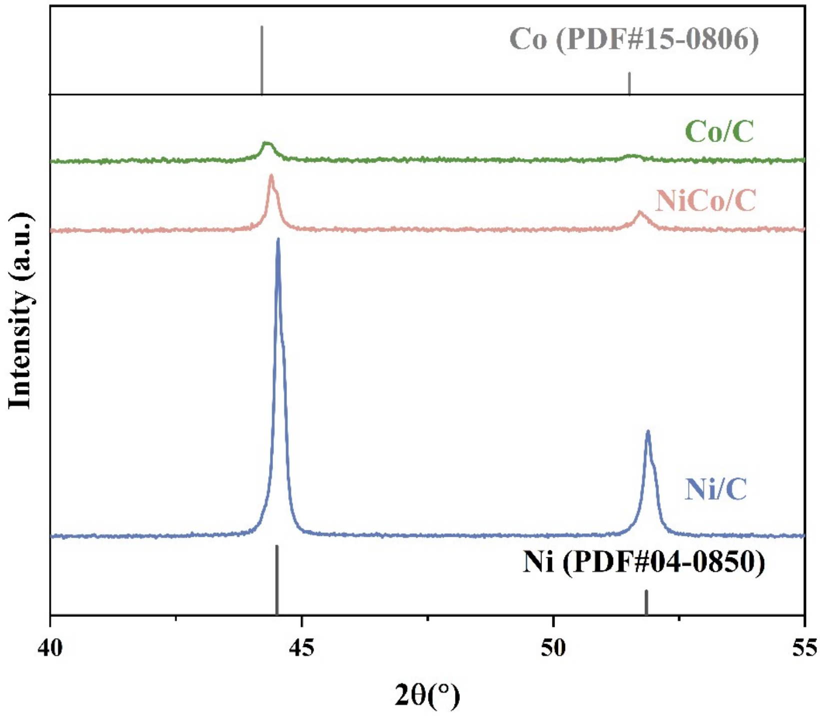

Figure S6. PXRD patterns of Ni/C、Co/C、NiCo/C, as compared to the corresponding powder pattern (Ni, PDF#04-0850, and Co, PDF#15-0806).

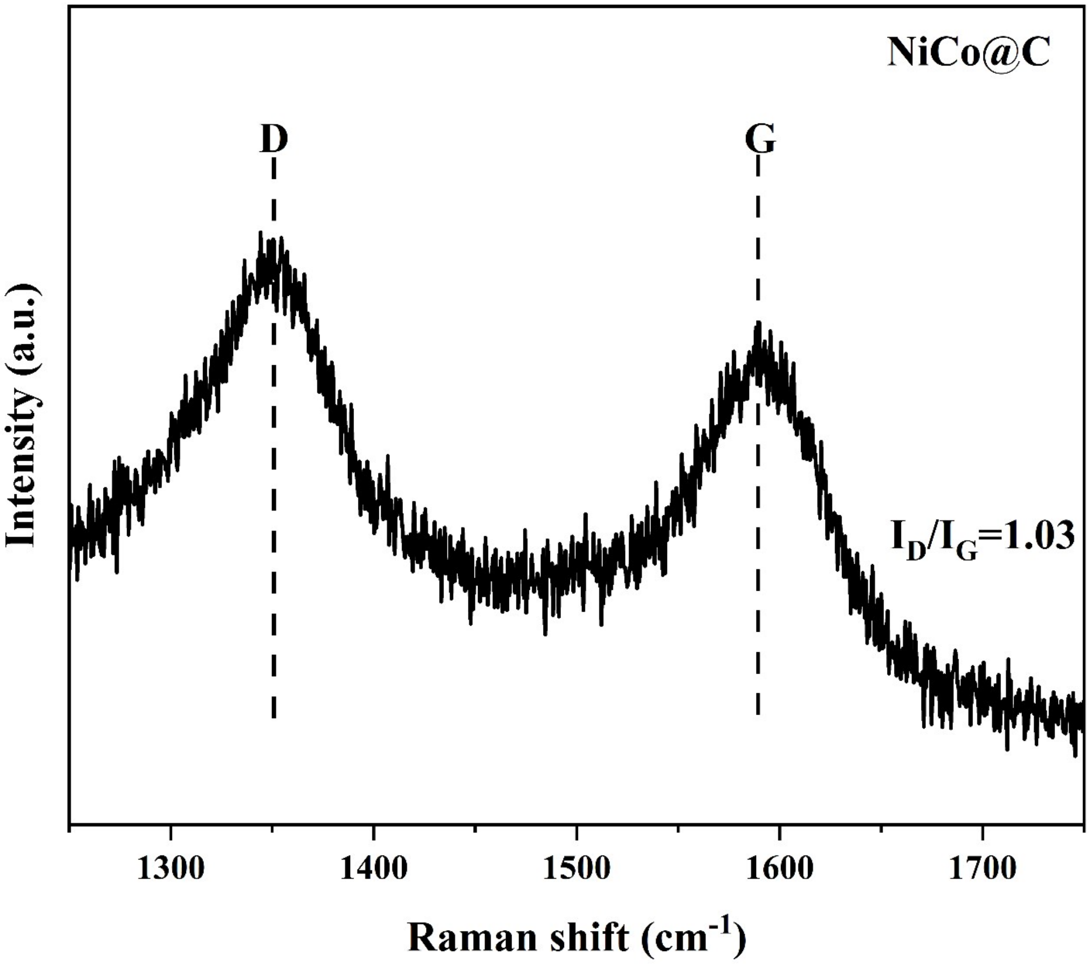

Figure S7. Raman spectroscopy of the NiCo/C.

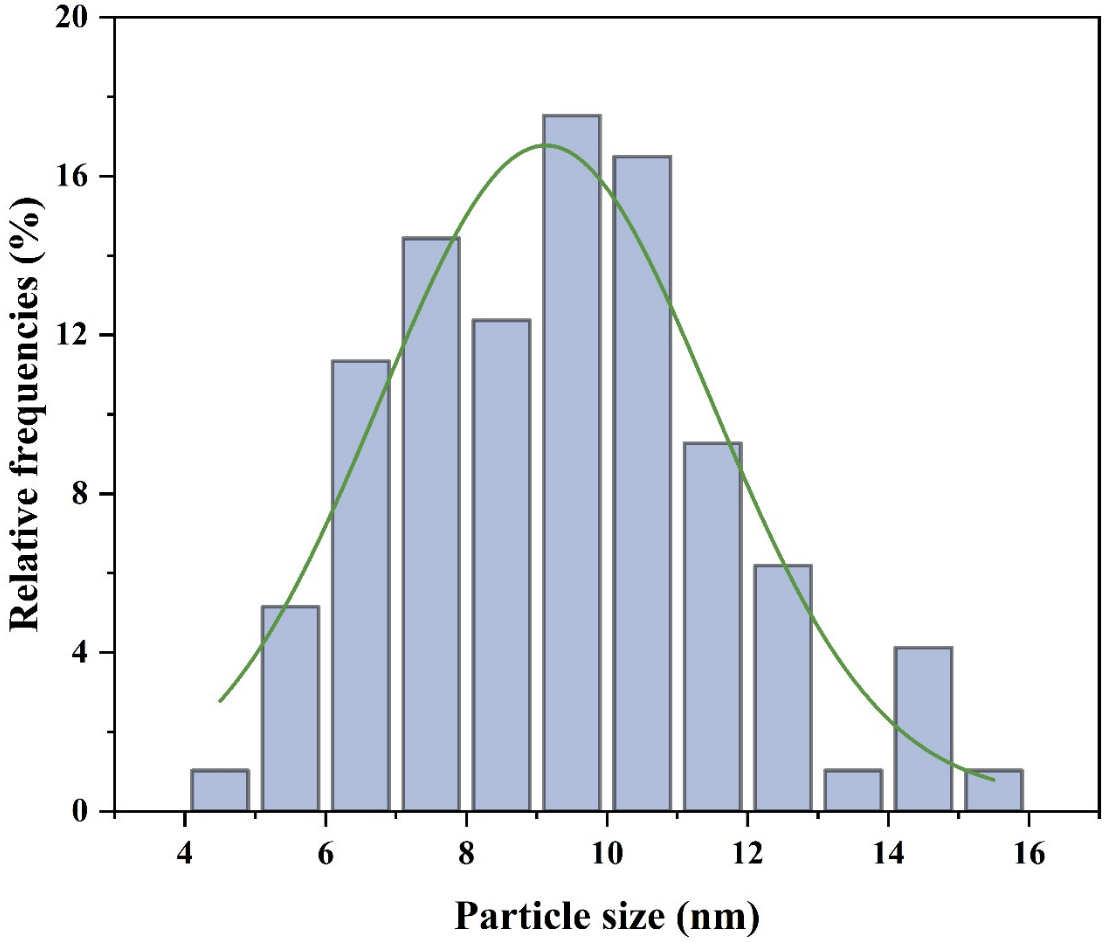

Figure S8. Particle size distribution of NiCo alloy nanoparticles in the NiCo/C.

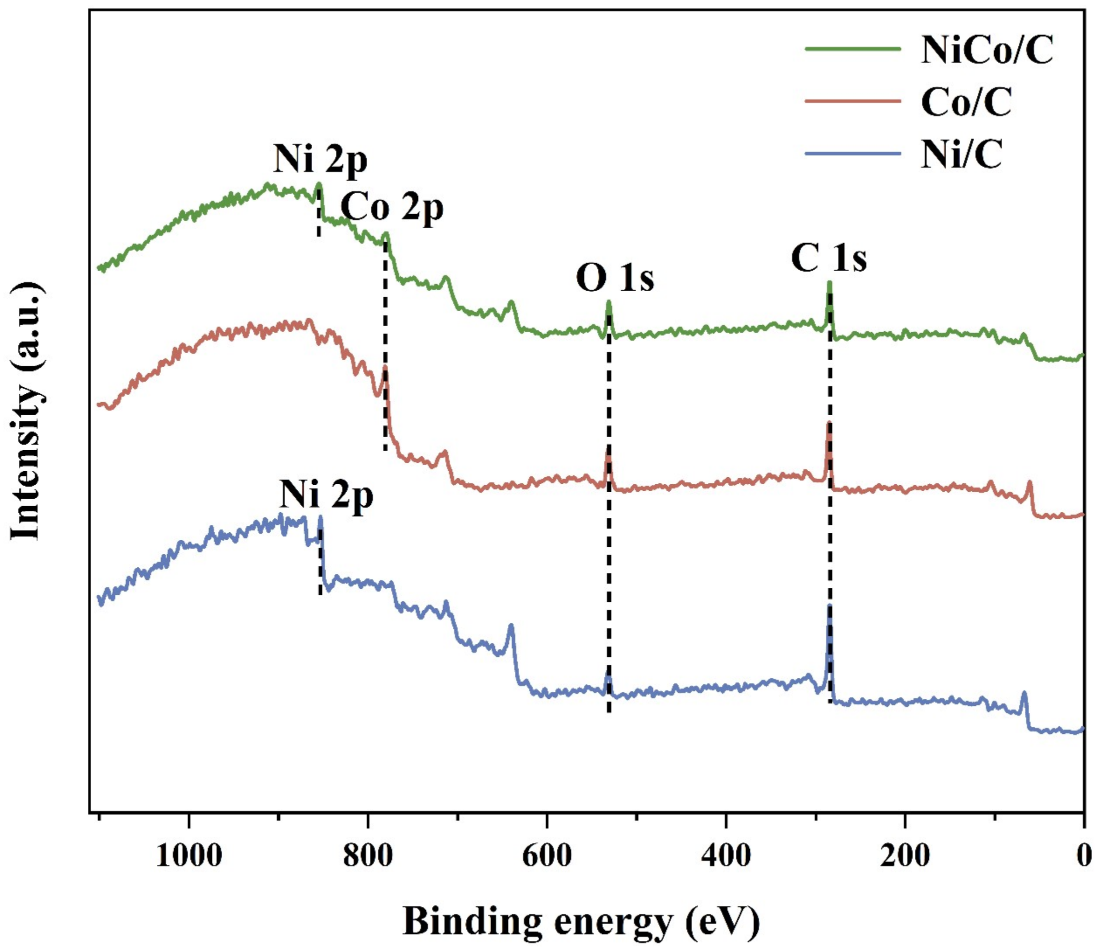

Figure S9. Full XPS spectra of Ni/C, Co/C and NiCo/C.

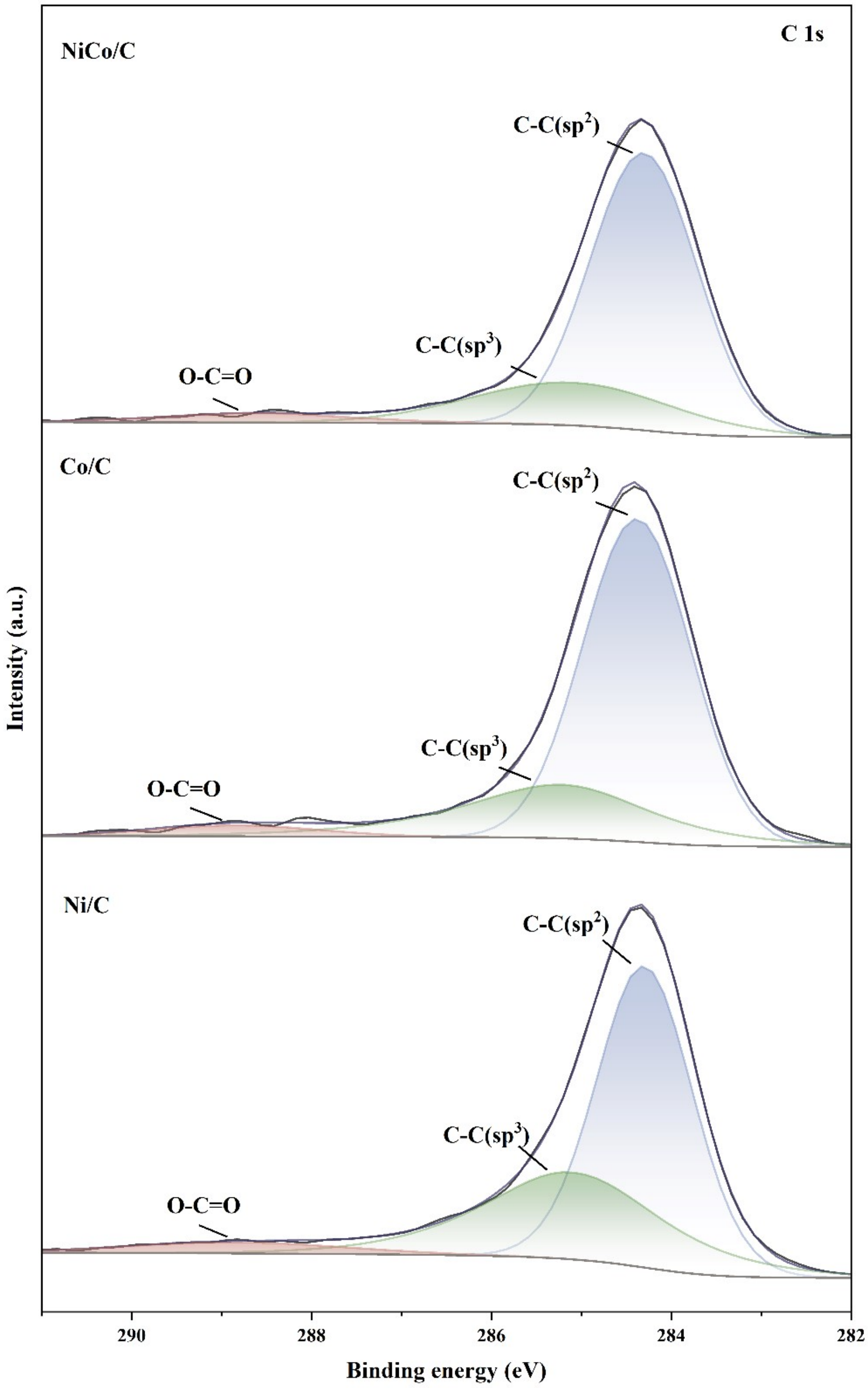

Figure S10. XPS spectra of C 1s for Ni/C, Co/C and NiCo/C.

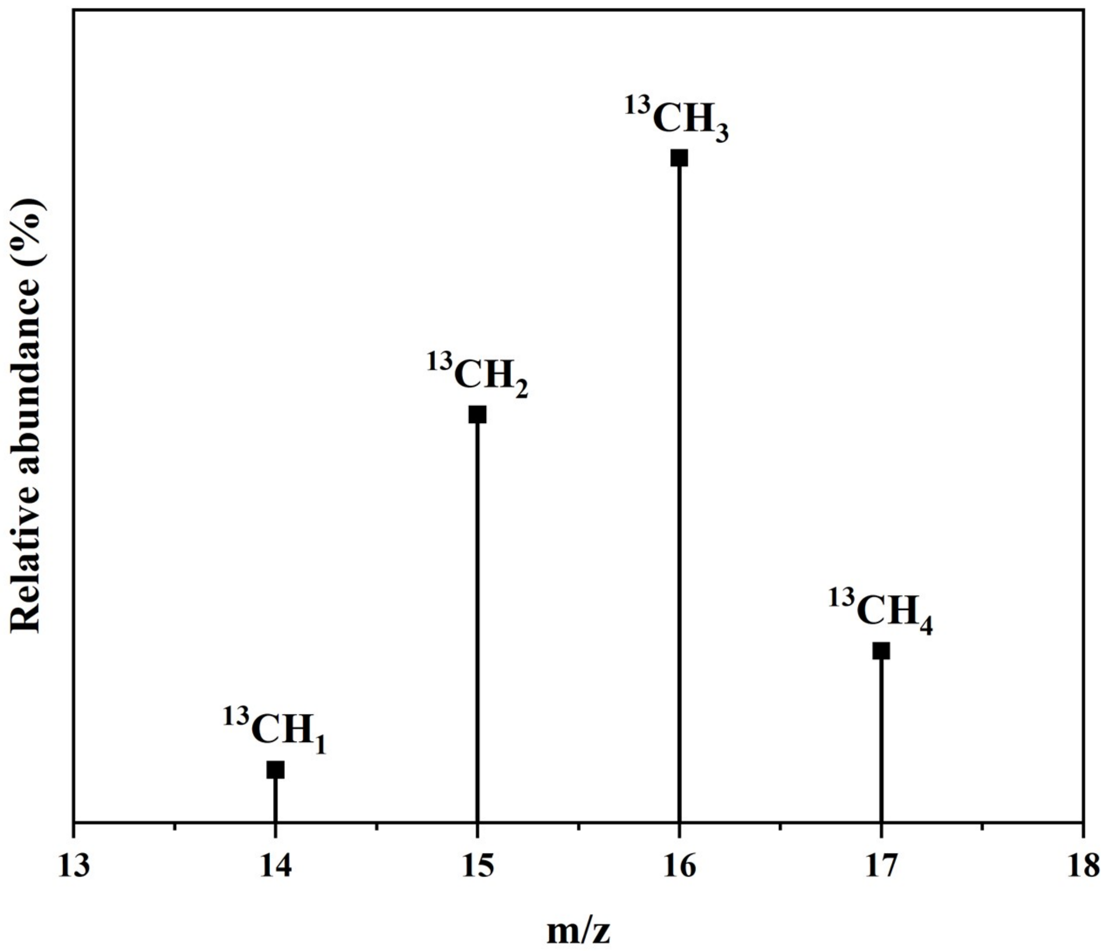

Figure S11. Mass spectra of ^{13}CO (inset) produced over NiCo/C.

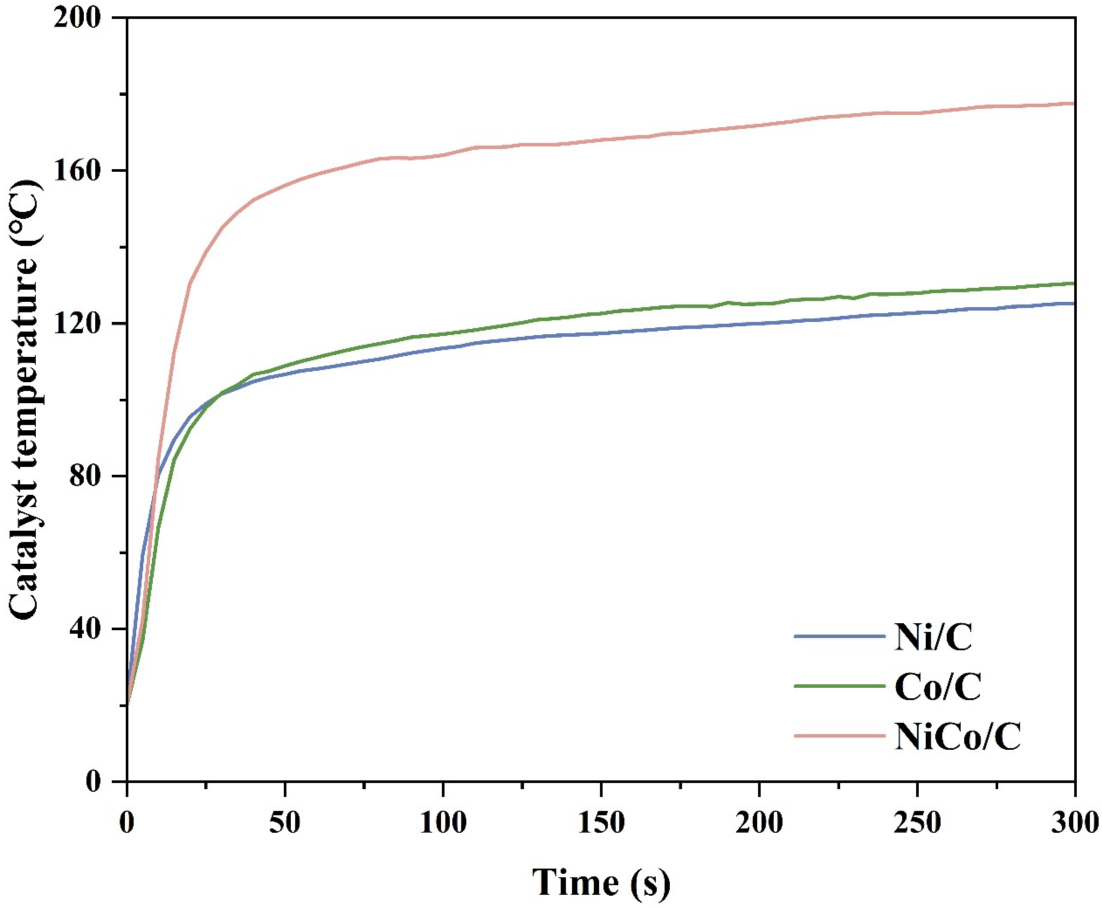

Figure S12. Temperature changes over Ni/C, Co/C and NiCo/C under light irradiation.

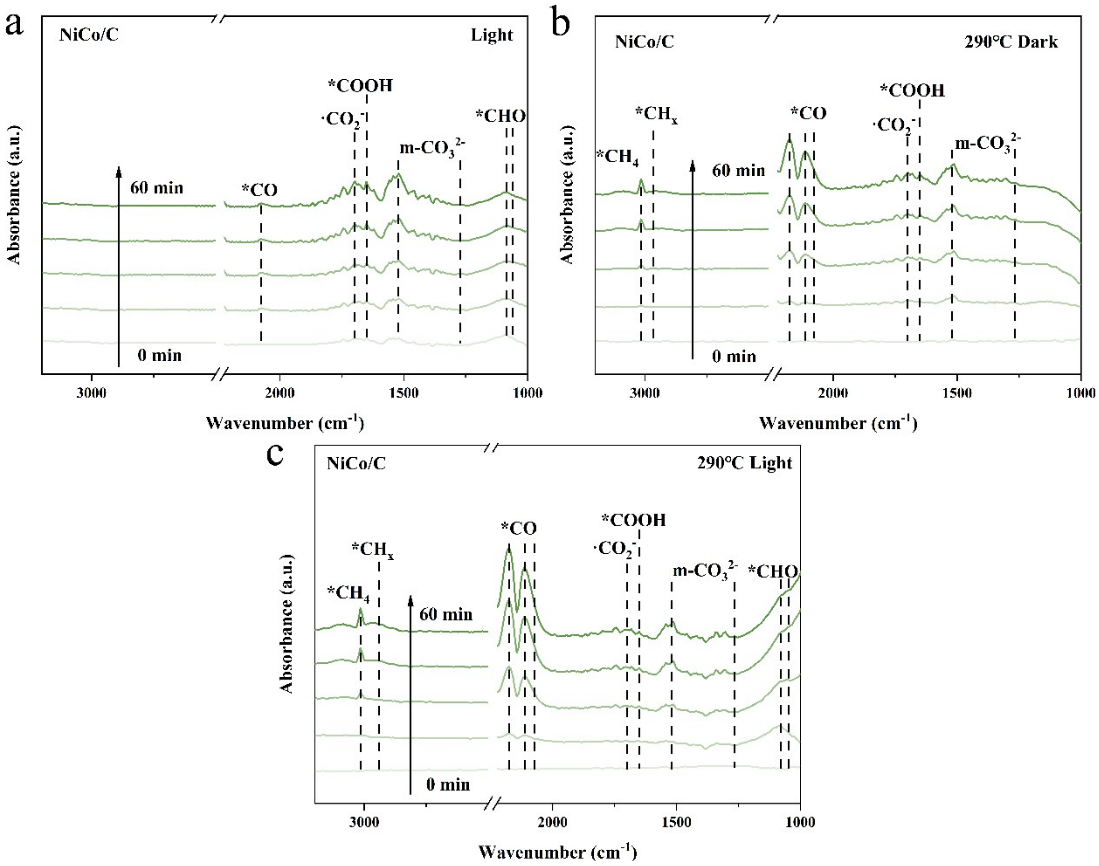

Figure S13. In situ DRIFTS spectra of NiCo/C catalyst a) under light irradiation, b) at 290 °C in dark, c) at 290 °C under light irradiation.

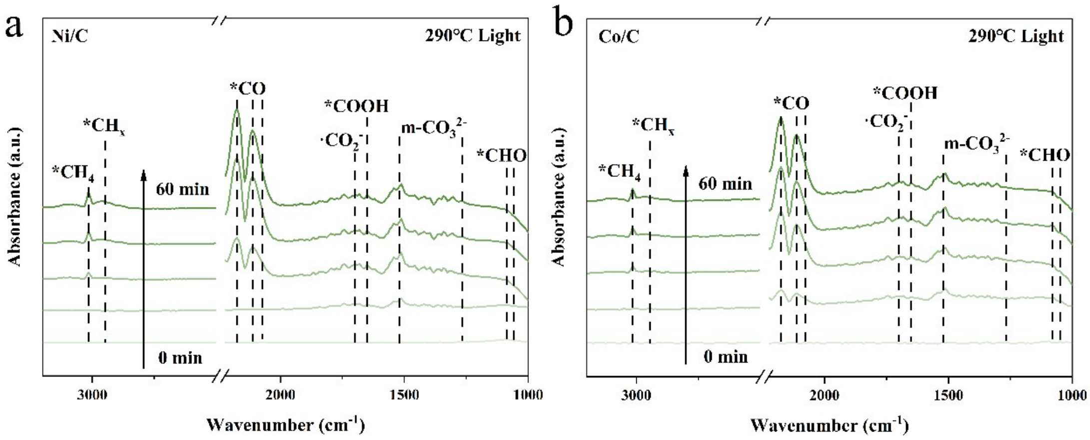

Figure S14. In situ DRIFTS spectra of a) Ni@C, b) Co@C catalysts at 290 °C under light irradiation.

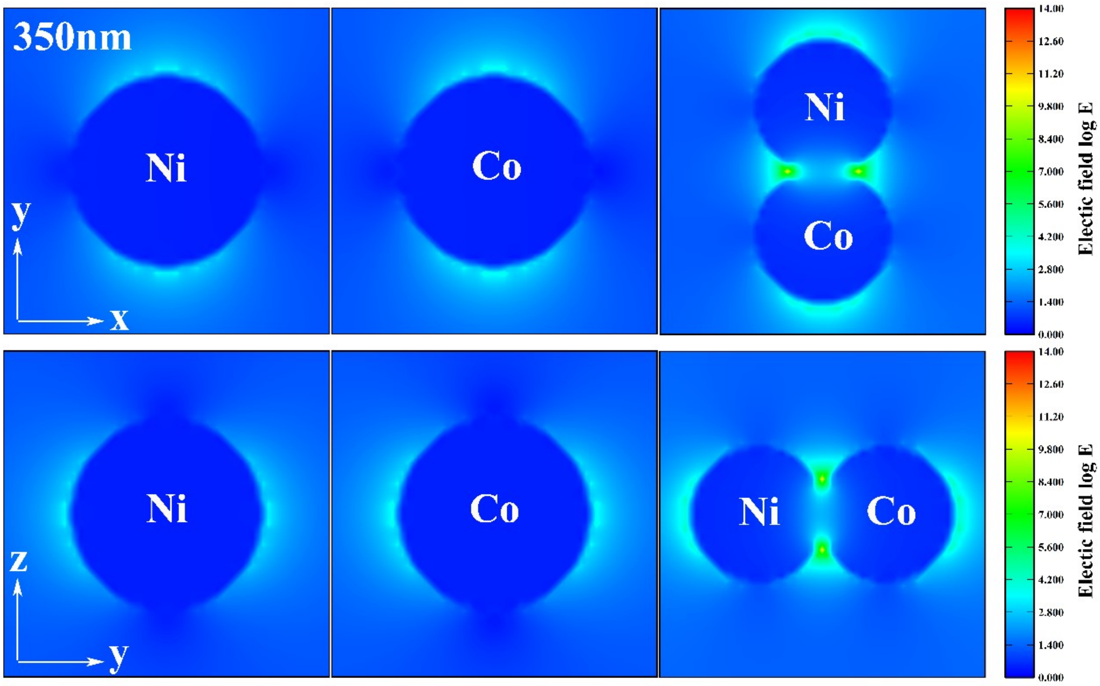

Figure S15. Induced electric field distributions of monometallic and bimetallic catalysts (Wave vector direction: x; Direction of polarization: y).

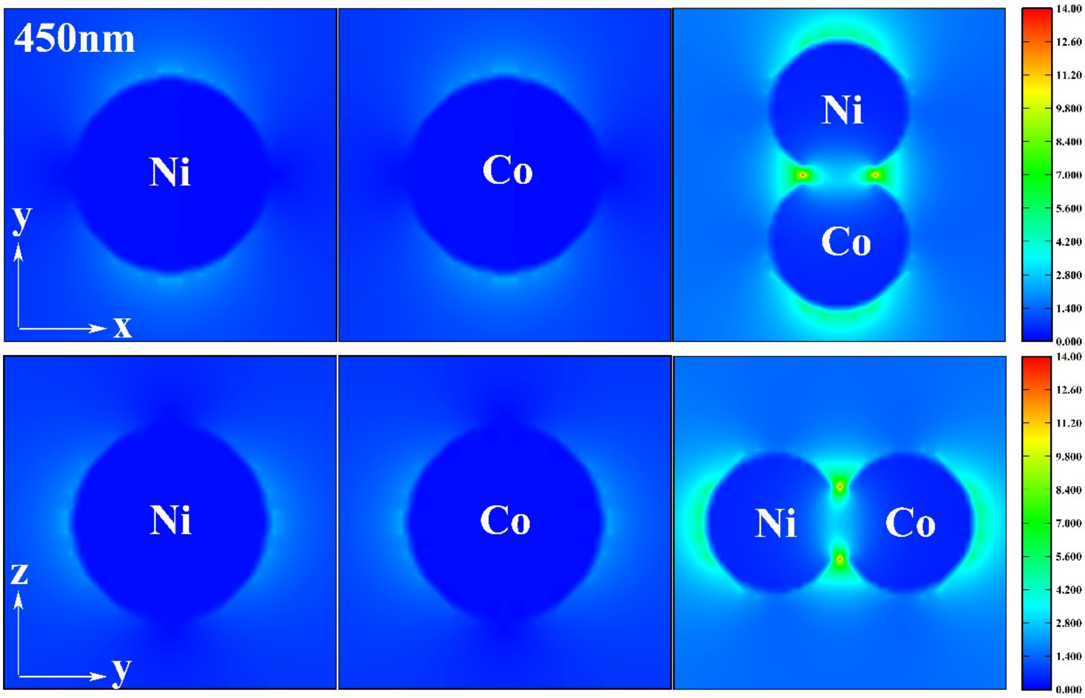

Figure S16. Induced electric field distributions of monometallic and bimetallic catalysts (Wave vector direction: x; Direction of polarization: y).

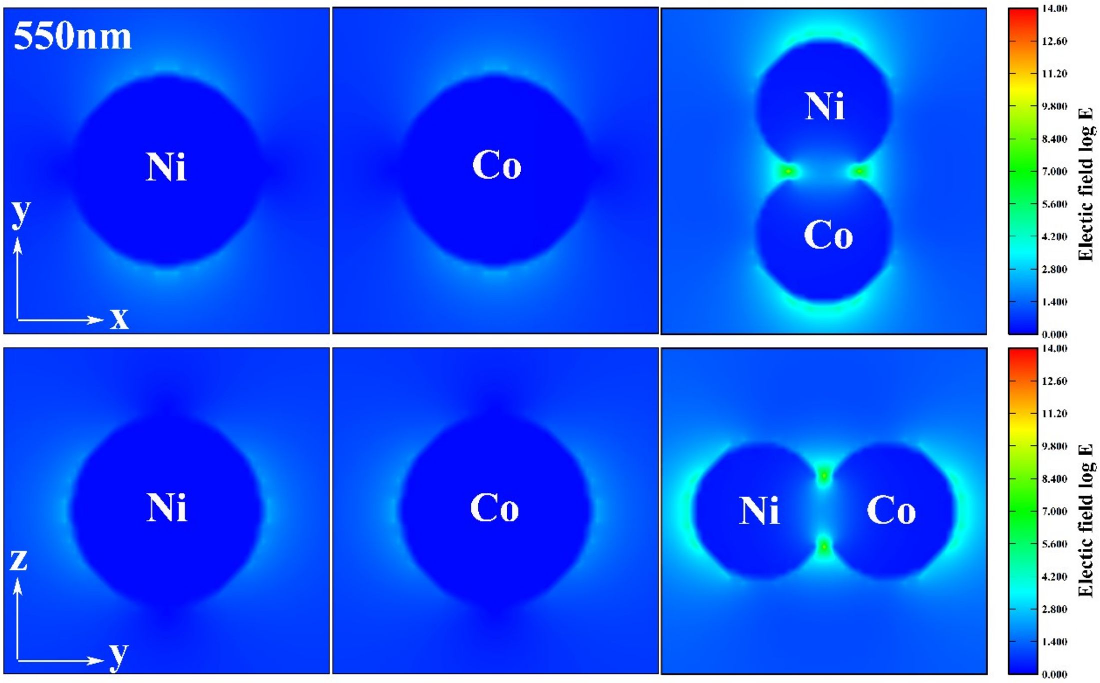

Figure S17. Induced electric field distributions of monometallic and bimetallic catalysts (Wave vector direction: x; Direction of polarization: y).

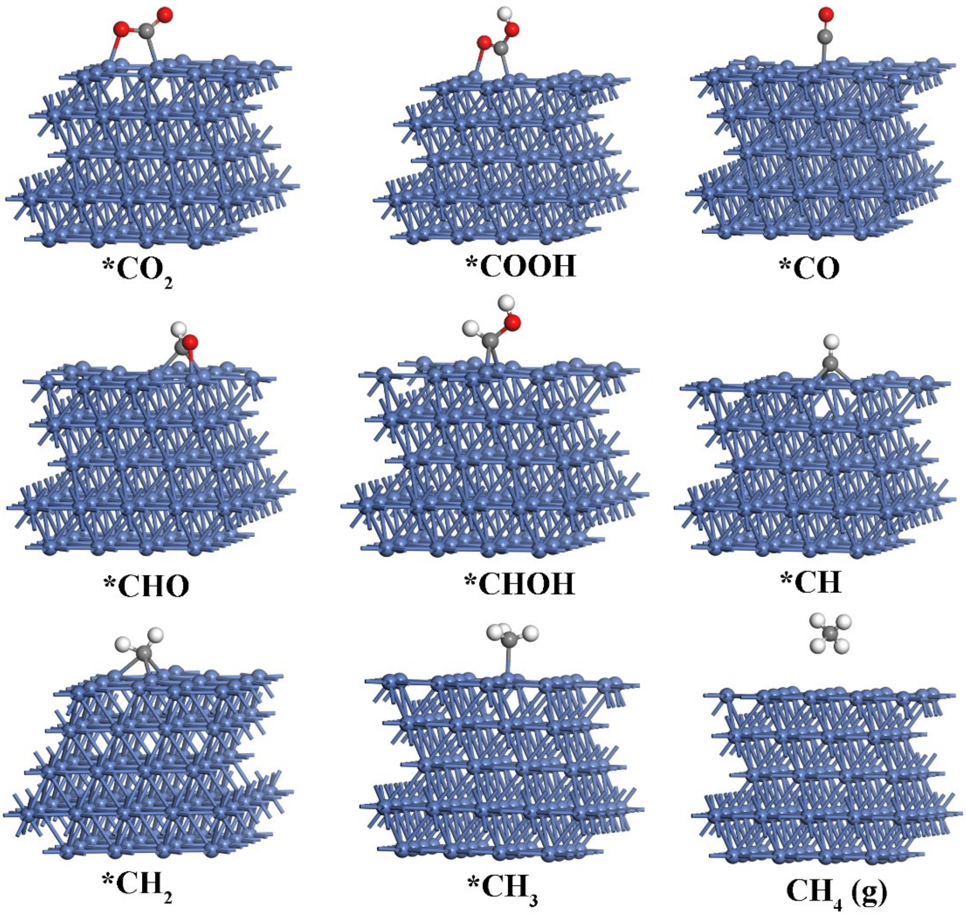

Figure S18. The optimized geometry of participating intermediates on Ni (111). The blue, grey, red and white spheres represent Ni, C, O and H atoms, respectively.

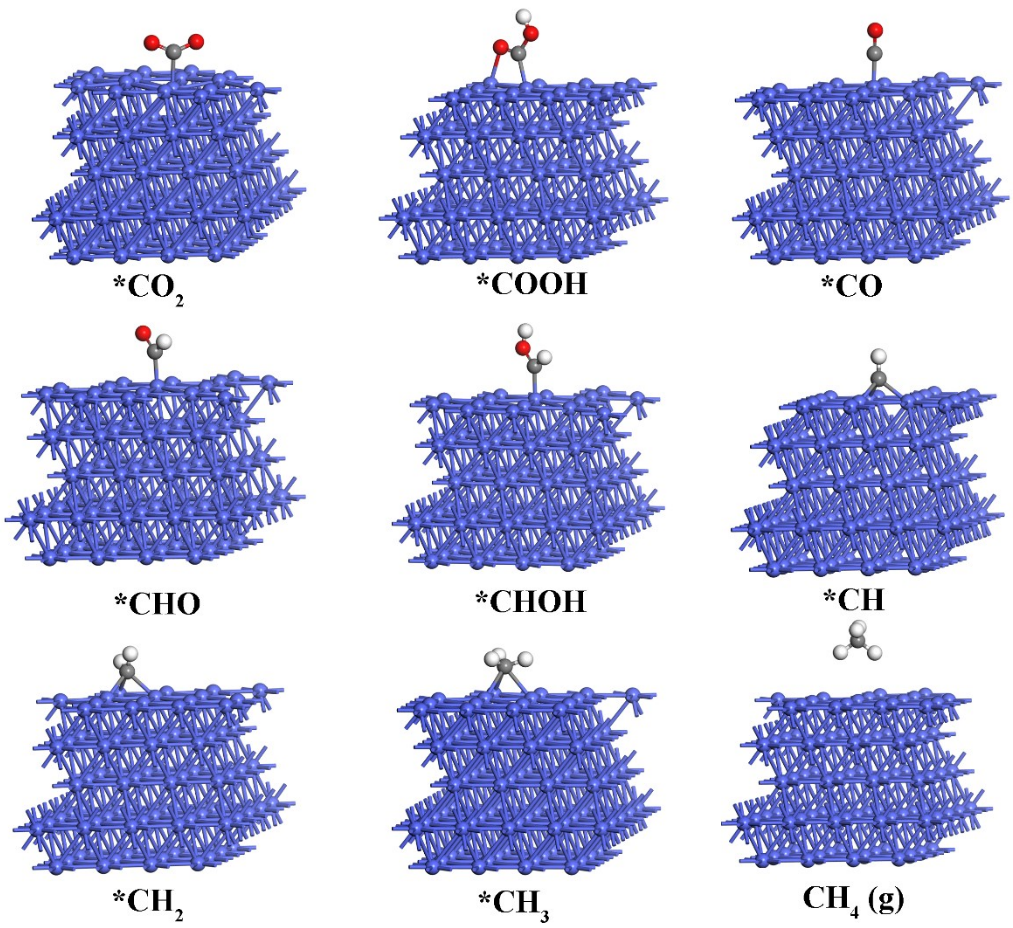

Figure S19. The optimized geometry of participating intermediates on Co (111). The purple, grey, red and white spheres represent Co, C, O and H atoms, respectively.

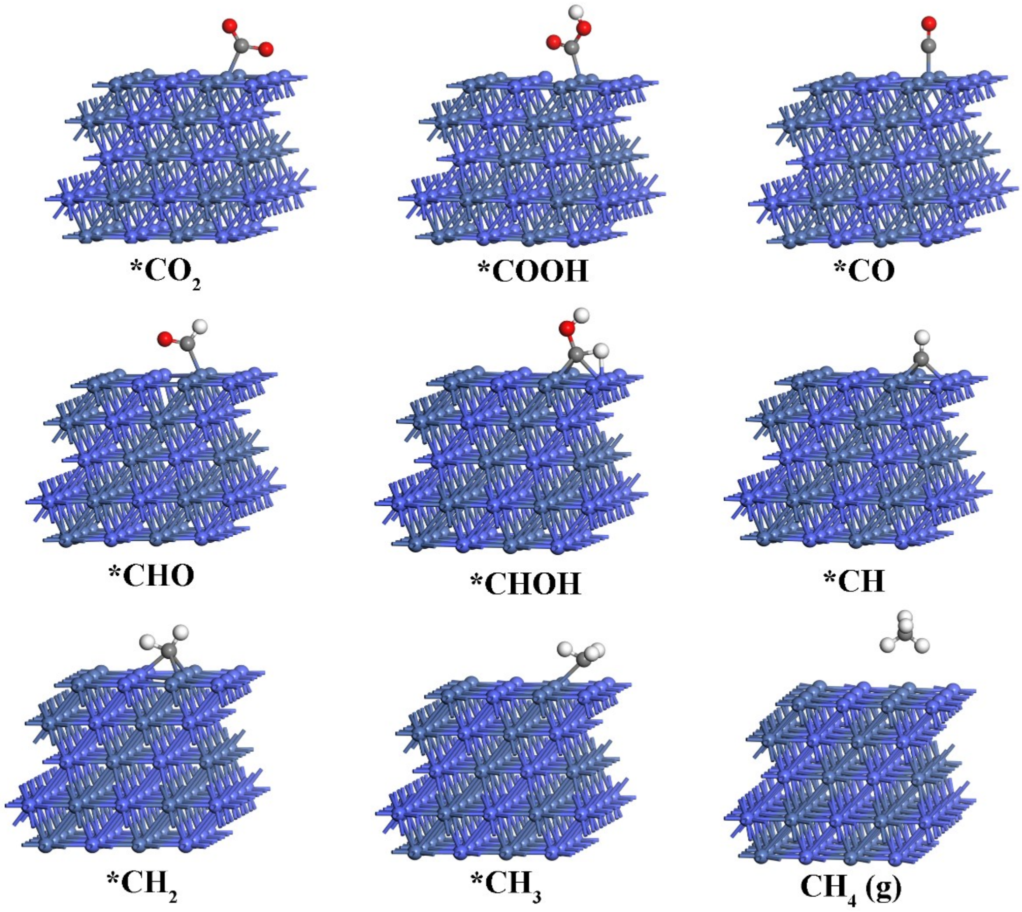

Figure S20. The optimized geometry of participating intermediates on Ni-Co (111). The blue, purple, grey, red and white spheres represent Ni, Co, C, O and H atoms, respectively.

Table S1. The comparison of catalytic activities with other reported catalysts for photo-thermal catalytic CO_2 hydro-methanation

Catalysis	Light source	External heating sources	Reactor type	Pressure (MPa)	Temperature (°C)	CO_2:H_2 rate	CH_4 rate (mmol g^{-1} h^{-1})	Selectivity (%)	Ref.
Ru/SiO_2	300W Xe lamp	Yes	Flow	0.1	300	1:6	35.1[a]	99.9	2
8Ni/TiO_2	375W IR Light	No	Flow	0.1	330	1:4	21.8[b]	99.5	3
8Ni/TiO_2	300W Xe lamp	No	Flow	0.1	198	1:4	6.3[a]	72.3	3
Ir/Uio-66	200-1000nm 300W Xe lamp	Yes	Flow	0.1	250	1:4	19.9[b]	95.0	4
Ni@SiXNS-EtOH	-	Yes	Flow	0.1	300	1:4	100.0[a]	90.0	5
Ru/TiO_2	500 W solar simulator	Yes	Flow	0.1	300	1:3	69.5[b]	-	6
Ni/Nb_2C	300W Xe lamp	No	Batch/Flow	0.1	321	1:1	72.5[b]	83%	7
Ru/H_xMoO_{3-y}	300W Xe lamp	No	Flow	0.1	140	1:1	20.8[b]	100	8
NiCo/C	300-2500nm 300 W Xe lamp 0.1 W/cm^2	Yes	Flow	0.1	290	1:3	67.8[a] 55.6[b]	98.0	This work

[a](mmol g_{metal}^{-1} h^{-1})
[b](mmol $g_{catslyst}^{-1}$ h^{-1})

Table S2. Energy barriers of elementary steps in CO_2 hydro-methanation reactions on Ni, Co and NiCo(111).

Entry	Species	Ni Eabs/eV	Co Eabs/eV	NiCo Eabs/eV
1	$CO_2(g) + * \rightarrow *CO_2$	0.60	0.56	0.45
2	$*CO_2 + *H \rightarrow *COOH$	-0.23	0.10	0.01
3	$*COOH + *H \rightarrow *CO + H_2O$	-0.81	-0.98	-0.82
4	$*CO + *H \rightarrow *CHO$	1.06	0.98	0.82
5	$*CHO + *H \rightarrow *CHOH$	0.03	0.54	0.11
6	$*CHOH + *H \rightarrow *CH + H_2O$	-1.18	-1.53	-0.9
7	$*CH + *H \rightarrow *CH_2$	0.14	0.11	0.04
8	$*CH_2 + *H \rightarrow *CH_3$	0.04	-0.36	-0.52
9	$*CH_3 + *H \rightarrow *CH_4$	-0.49	-0.28	-0.24
10	$*CH_4 \rightarrow CH_4(g) + *$	-0.33	0.06	0.06

1. S. Zhao, Y. Wang, J. Dong, C.-T. He, H. Yin, P. An, K. Zhao, X. Zhang, C. Gao, L. Zhang, J. Lv, J. Wang, J. Zhang, A. M. Khattak, N. A. Khan, Z. Wei, J. Zhang, S. Liu, H. Zhao and Z. Tang, *Nature Energy*, 2016, **1**, 16184.
2. C. Kim, S. Hyeon, J. Lee, W. D. Kim, D. C. Lee, J. Kim and H. Lee, *Nature Communications*, 2018, **9**, 3027.
3. Q. Li, Y. Gao, M. Zhang, H. Gao, J. Chen and H. Jia, *Applied Catalysis B: Environmental*, 2022, **303**, 120905.
4. Y. Tang, Z. Yang, C. Guo, H. Han, Y. Jiang, Z. Wang, J. Liu, L. Wu and F. Wang, *Journal of Materials Chemistry A*, 2022, **10**, 12157-12167.
5. X. Yan, W. Sun, L. Fan, P. N. Duchesne, W. Wang, C. Kübel, D. Wang, S. G. H. Kumar, Y. F. Li, A. Tavasoli, T. E. Wood, D. L. H. Hung, L. Wan, L. Wang, R. Song, J. Guo, I. Gourevich, F. M. Ali, J. Lu, R. Li, B. D. Hatton and G. A. Ozin, *Nature Communications*, 2019, **10**, 2608.
6. C. Wang, S. Fang, S. Xie, Y. Zheng and Y. H. Hu, *Journal of Materials Chemistry A*, 2020, **8**, 7390-7394.
7. Z. Wu, C. Li, Z. Li, K. Feng, M. Cai, D. Zhang, S. Wang, M. Chu, C. Zhang, J. Shen, Z. Huang, Y. Xiao, G. A. Ozin, X. Zhang and L. He, *ACS Nano*, 2021, **15**, 5696-5705.
8. H. Ge, Y. Kuwahara, K. Kusu, Z. Bian and H. Yamashita, *Applied Catalysis B: Environmental*, 2022, **317**, 121734.